Surface Characterization of 1-Butyl-3-methylimidazolium Br^-, I^-, PF_6^-, BF_4^-, $(CF_3SO_2)_2N^-$, SCN^-, $CH_3SO_3^-$, $CH_3SO_4^-$, and $(CN)_2N^-$ Ionic Liquids by Sum Frequency Generation

Selimar Rivera-Rubero and Steven Baldelli*

Department of Chemistry, University of Houston, Houston, Texas 77204

Received: November 5, 2005; In Final Form: January 17, 2006

Sum frequency generation spectroscopy, SFG, was used for the surface characterization at the gas−liquid interface of the 1-butyl-3-methylimidazolium cation combined with the following anions: Br^-, I^-, PF_6^-, BF_4^-, $(CF_3SO_2)_2N^-$ (imide), SCN^-, $CH_3SO_3^-$ ($MeSO_3$), $CH_3SO_4^-$ (MS), and $(CN)_2N^-$ (DCN). The SFG spectra obtained for the different ionic liquids were similar independent of the anion selected; therefore, a comprehensive analysis for the surface characterization of the ionic liquids' cation was focused only on the PF_6^- and Br^- anion combinations. For an accurate identification of the vibrational modes observed, FT-IR and Raman spectroscopy in combination with isotopic labeling with deuterium and polarized Raman spectroscopy was used. The cation orientation was determined by analysis of polarization-dependent SFG spectra. For a compound dried in a vacuum to $\leq 2 \times 10^{-5}$ Torr, the cation appears to be oriented with the ring laying flat along the surface plane and the butyl chain projecting into the gas phase independent of the anion identity.

Introduction

Organic solvents are used in large amounts for industrial processes, and because of their high volatility, they have become a focal point for an environmentally friendly solution. Room-temperature ionic liquids captured the attention of the scientific community as a good substitution for organic solvents in different systems such as liquid−liquid extraction, synthesis, and catalysis.[1−3] It is because of their high ionic conductivity, low vapor pressure, thermal stability, and wide electrochemical window that these compounds have become a novel solution to problems encountered with organic solvents.[4−7]

Ionic liquids are salts formed by an organic cation and a weakly coordinating anion. This weak interaction causes a decrease of the melting point compared to the most common inorganic salts, providing a range of salts that are liquid at room temperature if the right combination of ions is selected. Knowledge of the ions' influence on the behavior of the ionic liquids is necessary in the selection of the ion combination that suits the properties of the desired system. However, despite the use of ionic liquids in different applications, there have not been enough fundamental investigations to allow a complete understanding of its performance.

Imidazolium-based ionic liquids are commonly used given their easy manipulation and wide liquid range at room temperature when combined with different anions. These compounds are used in electrochemical and biphasic systems[8−13] such as solar cells,[14] liquid−liquid extraction,[12] and biphasic catalysis.[1,13] Furthermore, ionic liquids have promising applications in the separation of gases and gas captured from flue stacks.[15−19] Uptake of gas molecules is determined by the structure at the gas−liquid interface; therefore, to understand detailed mechanisms of uptake and absorption, the interfacial structure must be known at the molecular level.

Several surface studies that have been performed on ionic liquids are ion scattering,[20−22] neutron reflectometry,[23] surface tension,[21,24] sum frequency generation,[24−28] and atomistic simulation,[29] but there are variations in the results of the ionic liquid orientation at the gas−liquid interface. In this analysis, sum frequency generation, SFG, is used to determine the molecular orientation of the 1-butyl-3-methylimidazolium cation (BMIM) combined with Br^-, I^-, PF_6^-, BF_4^-, $(CF_3SO_2)_2N^-$ (imide), SCN^-, $CH_3SO_3^-$ ($MeSO_3$), $CH_3SO_4^-$ (MS), and $(CN)_2N^-$ (DCN) anions. This analysis will be compared with the results obtained by the different surface studies previously mentioned.

An important aspect for this analysis is the use of isotopic labeling with deuterium and polarized Raman spectroscopy to characterize the vibrational modes observed for the 1-butyl-3-methylimidazolium cation. Since the vibrational modes observed in the SFG spectra are used to determine the molecular orientation, it is essential to have an accurate peak assignment. Even with the information available for the vibrational modes of ionic liquids, there is not yet a complete set of data that allows a reliable assignment.[30−32] Recently, Conboy et al.[33] published an SFG analysis at the ionic liquid/SiO_2 interface and presented more complete peak assignments. To corroborate the vibrational assignments established by Conboy as well as eliminate any possible influences over the peak position by the ionic liquid/SiO_2 interface interaction, the vibrational modes observed in the SFG spectra were characterized using isotopic labeling in combination with IR and Raman spectroscopy as well as polarized Raman spectroscopy. The assignments established for *n*-alkanes by Snyder et al.[34−36] and Levin et al.,[37] and for methylimidazole by Pemberton et al.[38] and Carper et al.,[30] were combined with the experimental polarized Raman and isotopic labeled IR and Raman spectra to provide the different vibrational-mode assignments for the 1-butyl-3-methylimidazolium cation and allowed a definition of the peaks observed in the SFG spectra. This analysis provided a more thorough and reliable characterization of the cation at the liquid−gas interface.

10.1021/jp0563989 CCC: $33.50
Published on Web 02/14/2006

Background

SFG is a second-order nonlinear spectroscopy technique sensitive to molecules in a non-centrosymmetric environment such as the interface between two phases. The theory behind the SFG will not be covered; instead, the reader is referred to several reviews for a detailed discussion.[39−45]

In general, SFG only probes molecules with a preferential polar ordering. By overlapping a fixed-wavelength visible beam and a frequency-tunable infrared beam at the surface, a third beam is generated at the sum frequency of the incident beams. The intensity of the sum frequency generated light is proportional to the square of the induced polarization

$$I_{SF} \propto |P^{(2)} = \chi^{(2)}:\ E_{vis}E_{IR}|^2 \tag{1}$$

$$\chi^{(2)} = \chi_{nr} + \sum\left[\frac{N\langle\beta^{(2)}\rangle}{\omega_{IR} - \omega_q + i\Gamma_q}\right] \tag{2}$$

where E refers to the electric field of the visible and infrared input beams and $\chi^{(2)}$ is the second-order susceptibility tensor, which is dependent on the surface properties. The hyperpolarizability, $\beta^{(2)}$, contains the Raman polarizability and the infrared dipole transition, which are averaged over the molecular orientation, indicated by the brackets $\langle\ \rangle$. N is the number of modes contributing to the SFG signal. The ω_{IR} and ω_q refer to the frequency of the incoming IR and the normal mode of vibration, respectively, and Γ_q is the damping constant for the qth vibrational mode. The $\chi^{(2)}_{nr}$ arises from the nonresonant background of the surface.

By selecting different polarization combinations of the input and output light, the Cartesian components of the susceptibility tensor $\chi^{(2)}$ can be deduced. Since the magnitude of the measured susceptibility tensor is sensitive to the degree of the polar orientation of the molecules (eq 2), the information provided by the polarization analysis of the interface allows a determination of the molecular orientation with respect to the surface normal.[46]

Experimental Section

The synthesis and characterization of ionic liquids were performed by combining various procedures found in the literature.[4−6,47−50] All chemicals were from Sigma-Aldrich, unless otherwise specified, and were used without further purification. H NMR, FT-IR, Raman spectroscopy, mass spectroscopy (MS), and electrochemistry were used for characterization.

[BMIM][Br]. An equimolar mixture of 1-methylimidazole with 1-bromobutane was stirred and refluxed under nitrogen at ∼65 °C for 72 h. The product was purified by liquid−liquid extraction using ethyl acetate while keeping the system warm to avoid the crystallization of the salt. The final compound was dried under vacuum for about 48 h while stirring and heating at ∼80 °C until a pressure of $\leq 2 \times 10^{-5}$ Torr was reached.

[(d_9)-BMIM][Br]. The same procedure described for [BMIM][Br] was followed, but deuterated (d_9)-1-bromobutane from Cambridge Isotope Laboratories was used instead.

[BMIM][I]. The same procedure described for [BMIM][Br] was followed, but 1-iodobutane was used instead.

[BMIM][PF_6], [(d_9)-BMIM][PF_6]. The respective imidazolium bromides previously synthesized were mixed with HPF_6 at a molar ratio of 1:1.1 and stirred for at least 15 h. The product was washed 5 times with ice-cold deionized water and dried under vacuum for approximately 48 h while stirring and heating at ∼60 °C until a pressure of $\leq 2 \times 10^{-5}$ Torr was achieved.

[(d_3)-BMIM][PF_6]. For the synthesis of the ring deuterated at positions C2, C4, and C5, (d_3)-1-butyl-3-methylimidazolium hexafluorophosphate, the same procedure used by Wilkes[31] was followed. Approximately 50 mL (0.24 mol) of the non-deuterated ionic liquid was mixed with ∼2.4 g (17.3 mmol) of potassium carbonate (3 M) and ∼540 g (27 mol) of deuterated water (D_2O). The mixture was stirred while heating at 100 °C for 24 h. Synthesis was performed under nitrogen to avoid hydrogen exchange of the deuterated water (D_2O) with water (H_2O) from the air.

[BMIM][imide]. 1-Butyl-3-methylimidazolium chloride was synthesized following the same procedure as [BMIM][Br]. A small excess of Li($N(CF_3SO_2)_2$) was added in a 1:1.1 mol ratio and stirred for at least 15 h. The product was washed 5 times with ice-cold deionized water and dried under vacuum for approximately 48 h while stirring and heating at ∼60 °C until a pressure of $\leq 2 \times 10^{-5}$ Torr was reached.

[BMIM][BF_4]. The same procedure described for [BMIM][imide] was followed, but HBF_4 was used instead. To purify the product, dichloromethane was added to the ionic liquid prior to the cold washings.

[BMIM][SCN]. [BMIM][Cl] was mixed with a small excess of AgSCN in a mole fraction of 1:1.1 and stirred for approximately 1 h. Dichloromethane was added to the filtrate, and the mixture was cooled in the refrigerator overnight (temp ≈ 0 °C). The mixture was filtered again and dried under vacuum for approximately 48 h while stirring and heating at ∼60 °C until a pressure of $\leq 2 \times 10^{-5}$ Torr was reached.[48]

[BMIM][DCN]. A similar procedure described for [BMIM][SCN] was followed, but Ag($N(CN)_2$) was used instead.[50]

[BMIM][$MeSO_3$]. Synthesis of [BMIM][$MeSO_3$] was performed by following the procedure established by Robertson on his patent for preparation of ionic liquids.[49] The final product was dried under vacuum for approximately 48 h while stirring and heating at ∼60 °C until a pressure $\leq 2 \times 10^{-5}$ Torr was established.

[BMIM][MS]. $(CH_3)_2SO_4$ was added dropwise to a mixture of toluene and 1-butylimidazole. The temperature of the mixture was kept below 10 °C and the mixture kept under nitrogen until the reaction was completed. The final compound was washed 3 times with toluene and dried under vacuum for approximately 72 h while stirring and heating at ∼40 °C until a pressure of $\leq 2 \times 10^{-5}$ Torr was reached.

The desired ionic liquid was transferred to a spectroscopy cell constructed of glass with Kalrez O-rings and Teflon stopcocks. Prior to each experiment, the sample was evacuated to $\sim 1 \times 10^{-5}$ Torr while heating at 70 °C. To dry the sample, a glass vacuum line with liquid nitrogen traps and a diffusion pump was used. Approximately 1 h after the sample reached the base pressure, the cell was filled with argon gas just over the atmospheric pressure and detached from the line for the SFG analysis.

Since [BMIM][Br] is solid at room temperature, the spectroscopy measurements were conducted at a temperature of 80 ± 2 °C. Spectra for [BMIM][PF_6] were acquired at room temperature and at 80 ± 2 °C to observe any variation due to the difference in temperature. The sample was heated using heating tape wrapped around the spectroscopy cell and controlled with a variac. A type-K thermocouple in a glass sleeve was used for temperature readings directly in the ionic liquid.

The optical system consisted of a 1064-nm fundamental mode from an Ekspla picosecond Nd:YAG laser which was used to

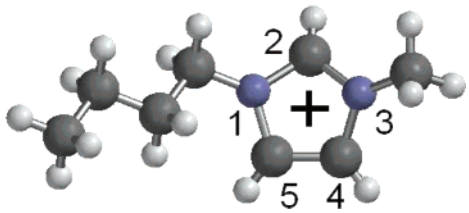

Figure 1. 1-Butyl-3-methylimidazolium.

pump a LaserVision OPG/OPA system, based on a set of KTP/KTA crystals, to create the tunable infrared light (2000−4000 cm^{-1}). The visible beam probes the surface at an angle of 50° from the surface normal with energy of 500 μJ and surface energy density of 28.5 mJ/cm^2. The infrared is at 60° with energy of 300 μJ and energy density of 8.5 mJ/cm^2 at 3000 cm^{-1}. A computer using the LabVIEW program controlled the electronics and the data collection.

Each spectrum was averaged over 5 or 10 scans of 20 shots/point at 1 cm^{-1}/s. The SFG data was corrected for infrared fluctuations, and the intensity was normalized to the CH_3 (sym) peak in the ssp spectrum, which is s for the sum frequency, s for the visible, and p for the infrared polarization. Polarization for the visible beam was changed using a half-wave (λ/2) plate antireflection coated for 532 nm supplied by CVI. The IR polarization was changed using a zero-order phase retardation plate (λ/2) supplied by ALPHALAS GmbH. The final SFG spectrum was fitted using Origin 6.0 Professional nonlinear curve fitting. Equation 2 was used as the fitting function with the instrumental weighting method, which allows a fit within the error of the curve.

Infrared and Raman spectra were recorded at room temperature on a Digilab FTS 7000 spectrometer in the 400−4000 cm^{-1} range. For the IR spectroscopy, a drop of dry ionic liquid was pressed between CaF_2 windows, and for the Raman, an NMR tube with the ionic liquid sealed under vacuum was used to acquire the spectra. Excitation was provided by a Nd:YAG laser at a wavelength of 1064 nm with a power of 500 mW and a resolution of about 4 cm^{-1}. Each spectrum was collected for 200 scans.

Polarized Raman spectra were acquired using a scanning Raman instrument with a Spex 1403 double monochromator equipped with a pair of 1800 grooves/mm gratings, a slit width of 3 cm^{-1}, and a Hamamatsu 928 photomultiplier detector. The 514.5-nm excitation line was provided by a Coherent Innova 90-6 Ar^+ ion laser with an output power of 50 mW. The samples were contained in an NMR tube sealed under vacuum and analyzed over the 2000−3300 cm^{-1} range.

Results and Discussion

The SFG spectra were acquired for the different combinations of ions and were found to be similar except for the [BMIM][MS] and [BMIM][$MeSO_3$] ionic liquids (Figure 2). These differences are only due to the presence of C−H vibrational modes arising from the anion. The presence of the same vibrational modes with similar relative intensities within the different polarization combinations indicates that under neat conditions the cation orientation is not affected by the anion identity. Therefore, the surface characterization will be focused on [BMIM][PF_6] and [BMIM][Br], since the deuteration and

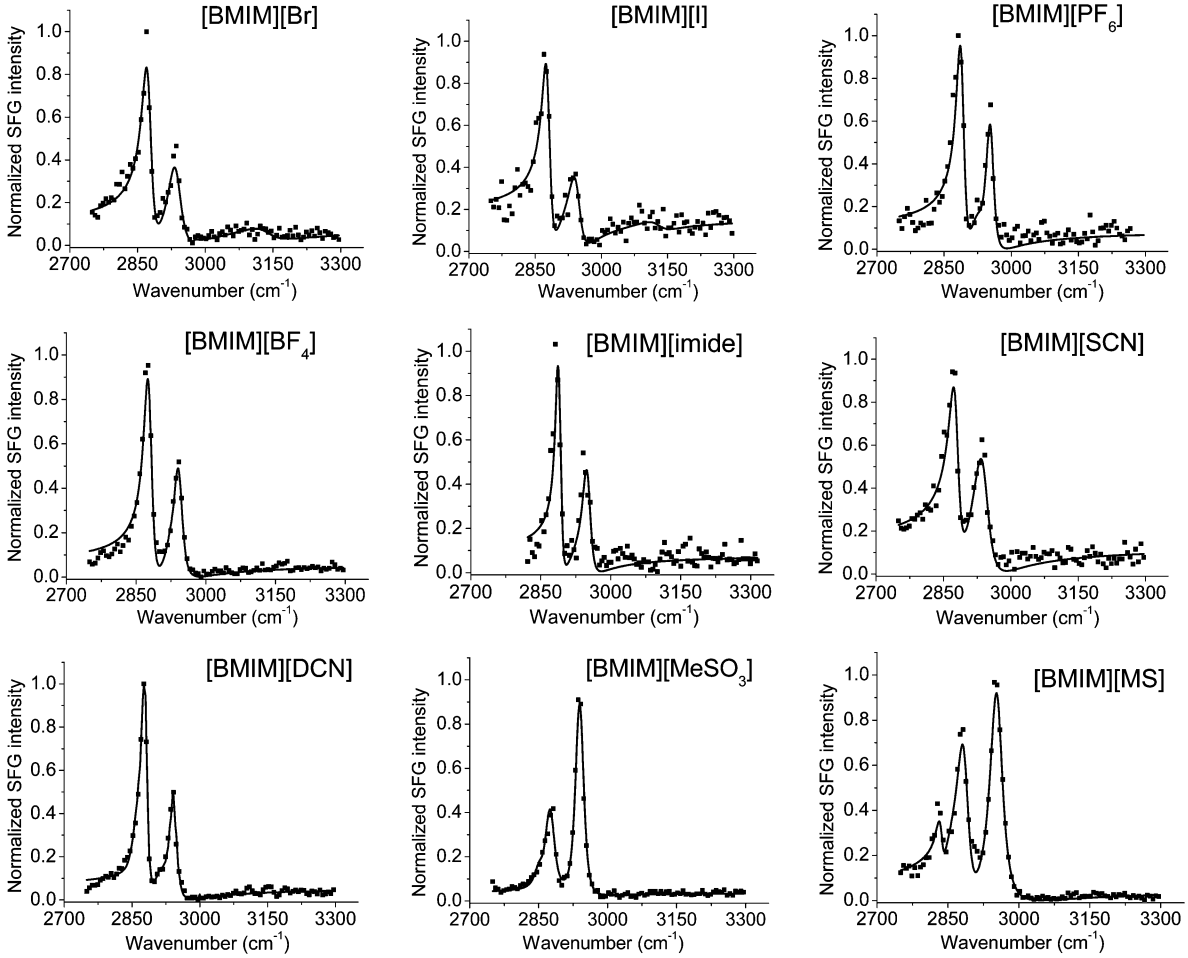

Figure 2. SSP polarized SFG spectra of 1-buyl-3-methylimidazolium cation combined with different anions (Br^-, I^-, PF_6^-, BF_4^-, imide$^-$, SCN^-, DCN^-, $MeSO_3^-$, and MS^-).

TABLE 1: Assignment for the CH Stretching Vibrations in the [BMIM]$^+$

frequency (cm^{-1})	IR assignment	Raman assignment	SFG ssp	SFG ppp	SFG sps
2065	CD_3 (sym)[a]	CD_3 (sym)			
2116	CD_2	CD_2			
2150	CD_2H (asym)[a]	CD_3 (asym)			
2212	CD_3 (asym)[a]	CD_3 (asym)			
2711	2δ (ring)	2δ (ring)[b]			
2825	2δ (ring)	2δ (ring)[b]			
2870	CH_3 (sym)[a]	CH_3 (sym)	√		
2910	CH_2 (asym)[a]	CH_2 (asym)			
2934	FR CH_3[a]	FR CH_3	√		
2968	CH_3 (asym)[a]	CH_3 (asym)		√	√
2970	N−CH_3 (sym)	N−CH_3 (sym)[b]			
2990	FR N−CH_3	FR N−CH_3[b]			
3035	N−CH_3 (asym)	N−CH_3 (asym)[b]			
3060	H-bonding interaction[c]	H-bonding interaction			
3110	C(2)−H[c]	C(2)−H			
3160	H−C(4)C(5)−H (asym)[c]	H−C(4)C(5)−H (asym)[b]			
3185	H−C(4)C(5)−H (sym)[c]	H−C(4)C(5)−H (sym)[b]			

[a] MacPhail, R. A.; Strauss, H. L.; Snyder, R. G. *J. Phys. Chem.* **1984**, *88*, 334. [b] Carter, D. A.; Pemberton, J. E. *J. Raman Spectrosc.* **1997**, *28*, 939. [c] ref 31.

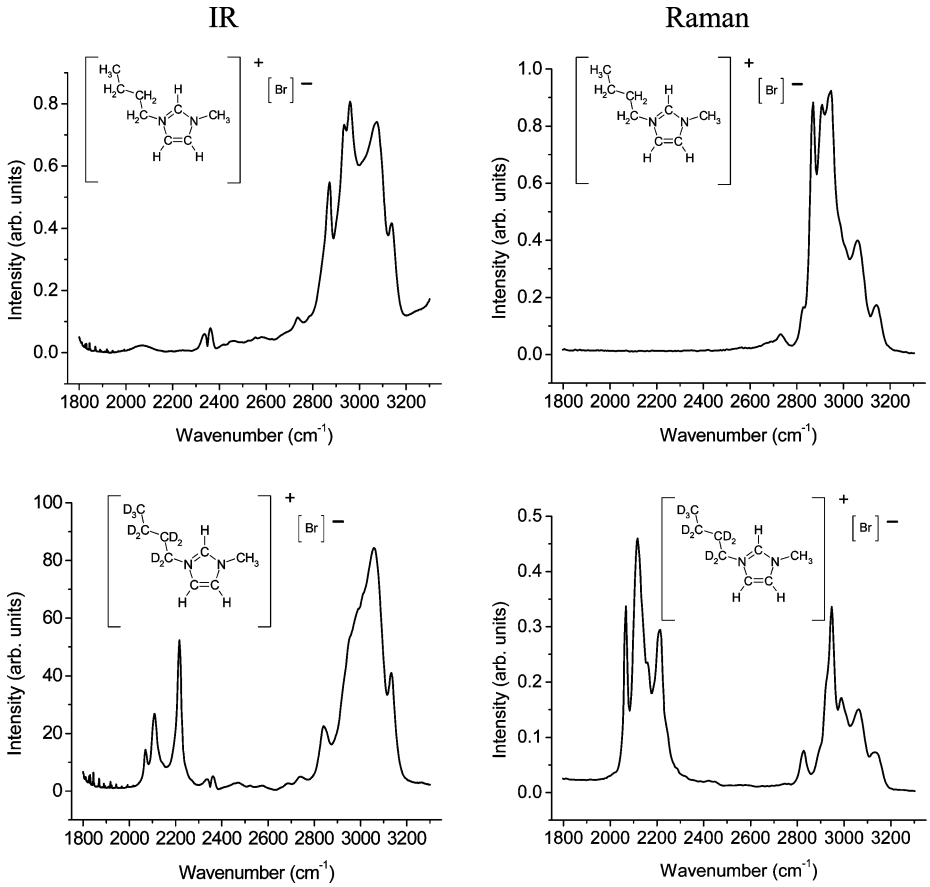

Figure 3. IR and Raman spectra for [BMIM][Br] and [(d_9)-BMIM][Br].

synthesis of these ionic liquids are straightforward and simple. Further, since the [BMIM][PF_6] is derived from [BMIM][Br], it provides two experiments from one (expensive) synthesis.

Peak Assignment. The imidazolium cation contains two methyl groups. One of the methyl groups is at the end of a butyl chain attached to one of the ring nitrogen atoms (position number 1); see Figure 1. The other methyl is directly attached to the nitrogen atom in position number 3 of the ring; see Figure 1. The different environments surrounding the methyl groups cause a difference in the frequency of the vibrations even though the local symmetry for both is assumed the same, C_{3v}. Isotopic labeling with deuterium in combination with the vibrational assignments found in the literature for *n*-alkanes[34−37] and methylimidazole,[30,38] were used to differentiate the stretching vibrations in the IR and Raman spectra of the two methyl groups as well as the vibrational modes of the imidazolium ring. Table 1 shows the vibrational assignment for the different peaks.

The IR and Raman spectra obtained for the neat salts [BMIM]-[Br] and [BMIM][PF_6] (see Figures 3 and 4) displayed five and six overlapped peaks between 2700−3200 cm^{-1}, respectively. Once the butyl chain was deuterated, some of the vibrational modes were red-shifted with four peaks in the region of 2000−2400 cm^{-1} in both the IR and Raman spectra.

Since spectra are acquired over the C−H frequency range and the vibrational modes arise from the same cation, it is not a surprise that the same peaks were observed for both the Br^-

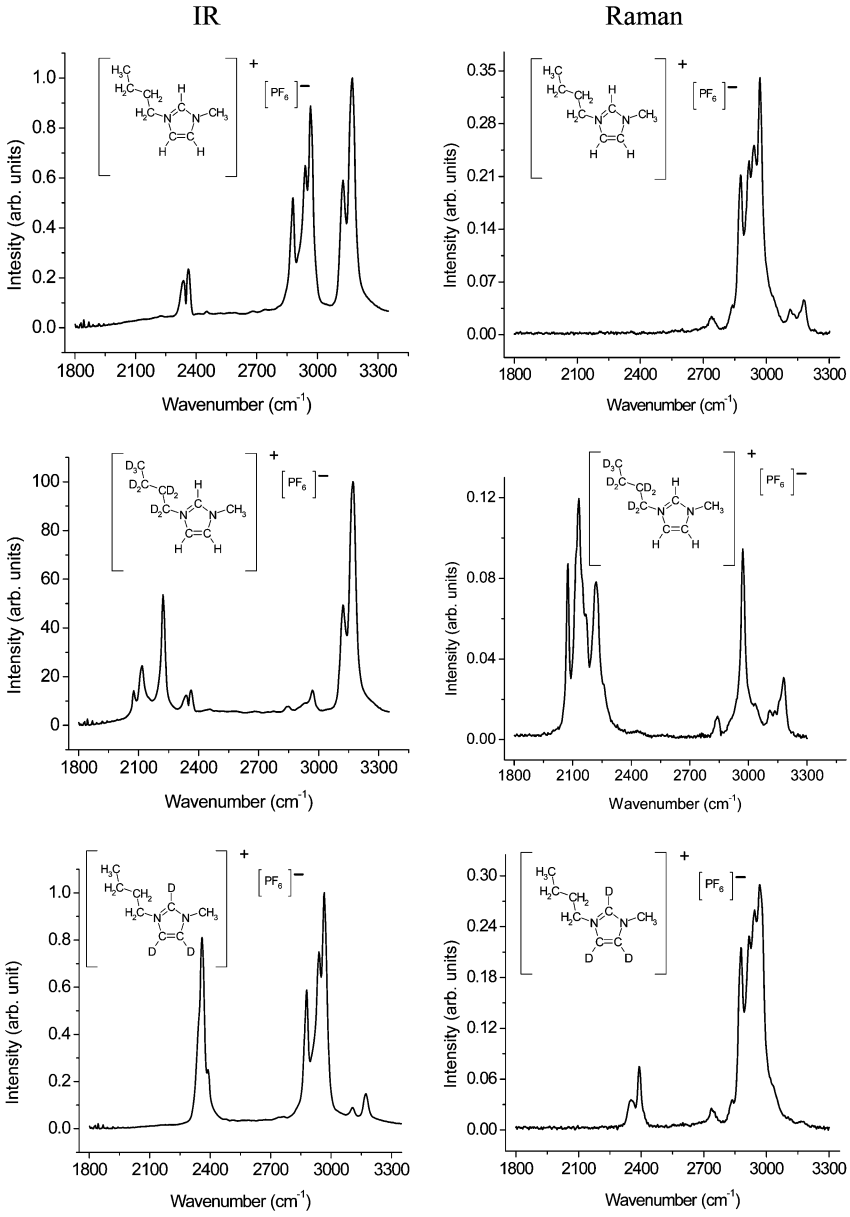

Figure 4. IR and Raman spectra of [BMIM][PF_6], [(d_9)-BMIM][PF_6], and [(d_3)-BMIM][PF_6].

and PF_6^- ionic liquids. Vibrational modes from the butyl chain seem to dominate the IR and Raman spectra. Bands at 2870 and 2968 cm^{-1} can be assigned as the CH_3 symmetric and antisymmetric modes, respectively.[34,37] A CH_2 (asym) peak appears at 2910 cm^{-1}.[34,37] There is also a Fermi resonance (FR) of the CH_3 (sym) with an overtone of the antisymmetric bending of the methyl at 2934 cm^{-1}.

After assigning the modes from the butyl chain, there were no peaks that could be clearly attributed to the $N-CH_3$. Therefore, a deuterated butyl chain was used in the synthesis, shifting the butyl chain peaks and allowing the identification of the $N-CH_3$ modes. The spectra of the deuterated ionic liquid, Figures 3 and 4, showed a strong peak at 2970 cm^{-1} with two shoulders at higher frequency and another two shoulders at lower frequency. Polarized Raman was used for better identification of the symmetric and antisymmetric modes. For $N-CH_3$, the symmetric mode is at 2970 cm^{-1}, and the antisymmetric mode is at 3035 cm^{-1} with the FR at 2990 cm^{-1}.[38] These assignments are in agreement with those stated by Conboy et al.[33] for the SFG spectroscopy of 1-alkyl-3-methylimidazolium-based ionic liquids. There are still two more peaks in the spectra that cannot be assigned to any of the vibrational modes of $N-CH_3$. These peaks arise from isotopic contamination of the deuterated butyl chain by hydrogen, which correlates with the 5% isotopic impurities for the (d_9)-1-bromobutane used as the starting material in the synthesis. According to the assignment of C−H stretching bands stated by Snyder,[34] the peaks at approximately 2905 and 2935 cm^{-1} are due to the C−H stretching of CHD and CHD_2, respectively.

For the imidazolium ring, a mode at 3110 cm^{-1} is assigned to the C(2)−H stretch, and the peaks between 3150 and 3200 cm^{-1} are the ring H−C(4)C(5)−H antisymmetric and symmetric modes.[31,38] These vibrational mode assignments agree with those found by Wilkes et al.,[31] who also found that there is a broad peak around 3060 cm^{-1} for the hydrogen bonding interaction of the anion with the ring protons. As seen in the IR spectra, Figures 3 and 4, this interaction is stronger for Br^- than for PF_6^-. The spectra of the deuterated-d_3 ring confirmed that the peaks previously labeled belong to the C−H vibrational modes of the ring, as the peaks shifted to the region of 2340−2390 cm^{-1}.

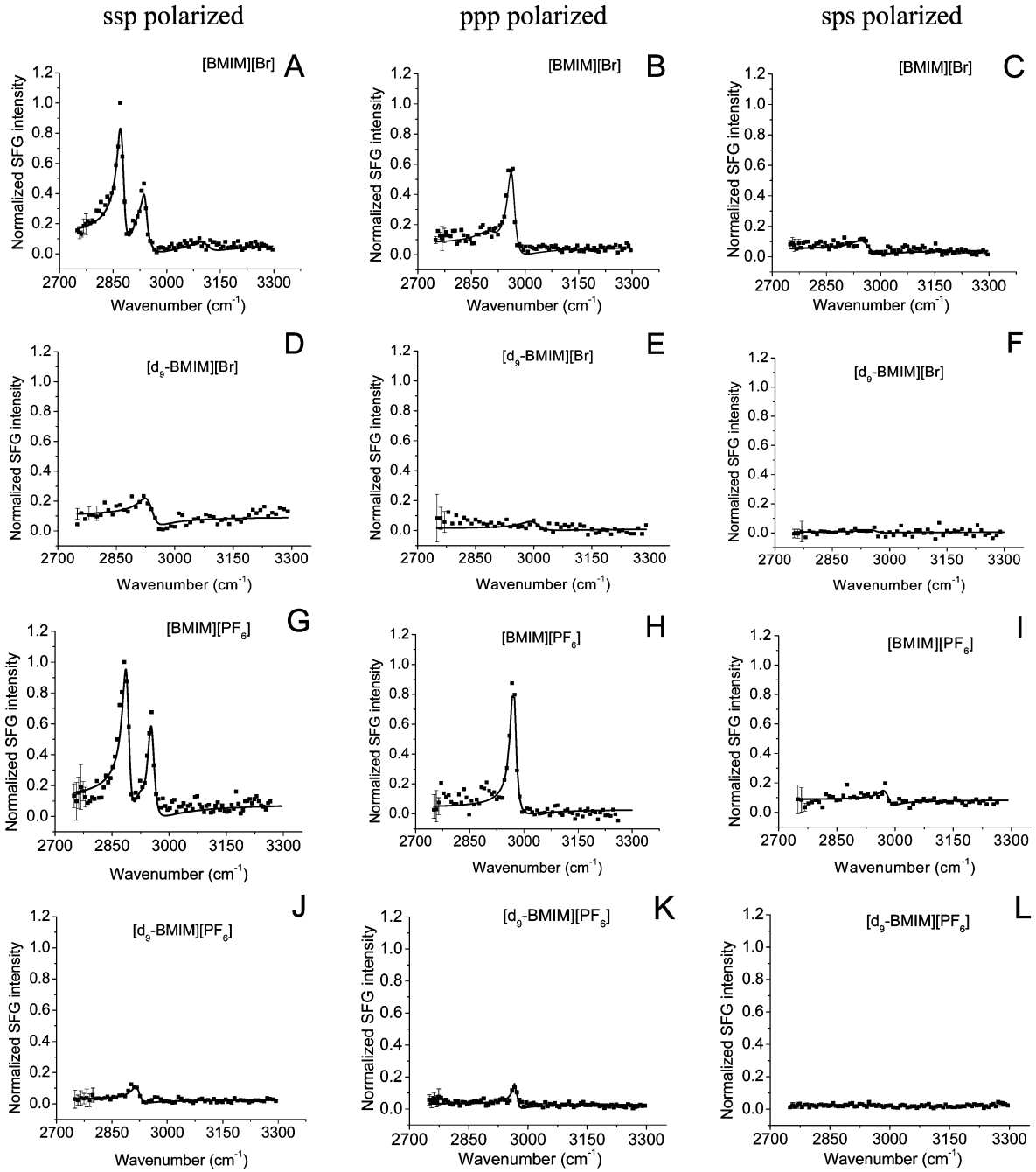

Figure 5. SFG spectra of [BMIM][Br], [(d_9)-BMIM][Br], [BMIM][PF_6], and [(d_9)-BMIM][PF_6] for the different polarizations.

The SFG spectrum was obtained for the C−H region of 2750−3300 cm^{-1}, and by using the peak assignment established from the IR and Raman spectra, the SFG resonances were identified.

In Figure 5A,G, the ssp spectra for [BMIM][Br] and [BMIM]-[PF_6] showed two resonances at 2880 and 2945 cm^{-1}, which can be assigned to the symmetric and FR modes of the butyl CH_3, respectively, while a third resonance, observed only for [BMIM][Br] at 3100 cm^{-1}, is assigned to the interaction peak previously identified in the IR spectrum by Wilkes et al.[31] The ppp spectra, Figure 5B,H, as well as the sps, Figure 5C,I, showed only one resonance at 2970 cm^{-1} assigned to the CH_3 (asym) mode of the butyl chain.

Deconvolution and assignment of the vibrational modes for both methyl groups of the imidazolium is particularly important when the peak intensities are used in the analysis to establish the molecular orientation. Intensities from the N−CH_3 modes can be easily confused with the CH_3 (asym) mode because of the similar frequency, providing an inaccurate analysis of the peak. Another important fact that has to be considered when analyzing the spectra is that the line shape of the SFG spectra is defined by the square modulus of eq 2. This equation consists of the nonresonant background and the resonant vibrational modes. The shape of the spectra will be influenced by the interferences of the vibrational modes with each other as well as with the nonresonant contribution. Therefore, the amplitudes of the peaks interfere with each other, affecting their intensity and shape. The SFG spectra acquired showed only resonances from the butyl CH_3. To confirm that the absence of any vibrational mode from the N−CH_3 is due to its orientation and not to any destructive interference with either the CH_3 (FR) or CH_3 (asym) modes, the SFG spectra of [(d_9)-BMIM][Br] and [(d_9)-BMIM][PF_6] were acquired.

The SFG spectra of the deuterated butyl chain ionic liquids [(d_9)-BMIM][Br] and [(d_9)-BMIM][PF_6] displayed one small peak at 2920 cm^{-1} in the ssp spectra, Figure 5D,J, while the ppp polarization exhibits a peak at 2970 cm^{-1} as seen in Figure 5E,K, with no peak for the sps, Figure 5F,L. Following the assignment stated previously, the resonance observed at 2920 cm^{-1} in the ssp polarized spectra does not agree with any of the resonances from the N−CH_3 but with that of the C−H stretch from the isotopic impurity CHD_2. On the other hand, for the ppp polarized spectra, the resonance observed at 2970 cm^{-1} is at the corresponding frequency of the N−CH_3 (sym), but there are two points that have to be considered before making any assignment. First, the polarization selection rules for a C_{3v} group, such as CH_3, do not allow the symmetric mode to be more intense in the ppp than in the ssp.[51] In other words, if the peak observed in the ppp spectra was that of the N−CH_3 (sym), it should also be seen in the ssp spectra many times stronger than that of the ppp. Second, if the mode is considered to be arising from some isotopic impurity of hydrogen, its identification is not possible by using the C−H region of the IR or Raman spectra, given that its frequency is overlapped by the N−CH_3 (sym) mode. Hence, to determine if the peak is from some hydrogen contamination and what type of C−H contamination is observed, its corresponding C−D vibrational modes are used instead. Using the assignment stated by Snyder,[34] a peak at 2970 cm^{-1} could be from the C−H antisymmetric mode of the CH_2D. If this was the case, then its corresponding C−D stretch should be observed at ∼2168 cm^{-1}. From the analysis of the C−D region of the deuterated Raman spectra, Figure 4, a peak is observed at ∼2165 cm^{-1}, which confirms that the peak seen in the ppp spectra is the C−H antisymmetric mode from CH_2D. With the two peaks identified as isotopic impurities of the deuterated butyl chain by hydrogen, it is reasonable to say that no peaks from the N−CH_3 are observed in the SFG spectra for the different polarization combinations. The absence of the N−CH_3 peak is later used as support for the orientation found for the imidazolium cation discussed below.

The deuterated ring [(d_3)-BMIM][PF_6] spectra for the different polarizations were not distinguishable from those of the ionic liquid [BMIM][PF_6], supporting the idea that there was no resonance from the ring C−H vibrational modes as previously mentioned.

By comparing the SFG spectra of the $[BMIM]^+$, [(d_3)-$BMIM]^+$, and [(d_9)-$BMIM]^+$, the peaks observed are confirmed to be solely from the butyl CH_3, and the orientation of the imidazolium cation at the surface can be estimated.

Even though this analysis was focused over [BMIM][Br] and [BMIM][PF_6], it is important to mention again the SFG spectra of [BMIM][MS] and [BMIM][$MeSO_3$]. The anion vibrational modes observed in the SFG spectra are of extreme importance, since they indicate the presence of the anion at the surface as well as the cation. These results are in accordance with the ion distribution at the surface previously found by other groups.[20,21]

Orientation Analysis. To determine the orientation of the molecules at the surface, the molecular coordinate (*a*, *b*, *c*) is related to the surface coordinate (*x*, *y*, *z*), Figure 7. The same coordinate definition used by Hirose[43,44] was applied in this analysis. In the surface coordinate, the *x*−*y* plane is defined as the surface plane with the *x*−*z* plane as the plane of incidence of the laser beams. For the molecular coordinate, the *a*−*c* plane is defined to coincide with the σ_v plane for the C_{3v} methyl of the alkyl chain with the *c* axis along the methyl C_3 axis; see Figure 7. With these axis definitions, the orientation of the molecule for a δ-distribution function is expressed by the tilt (θ) angle of the *c* axis with respect to the *z* axis and the twist (φ) along *c*. Orientation in the *x*−*y* plane (defined by the χ angle) is assumed to be isotropic for the liquids and therefore is not referred to in the molecular orientation description.

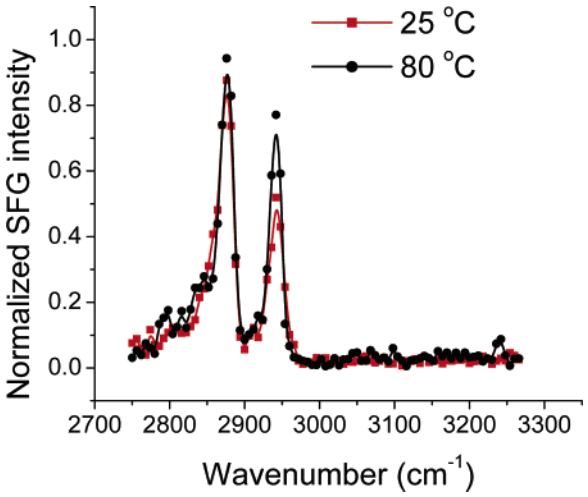

Figure 6. SFG of [BMIM][PF_6] at 25 °C and 80 °C.

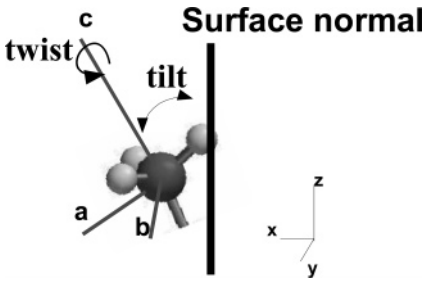

Figure 7. Description of the molecular coordinate axis (*a*, *b*, *c*) and surface coordinate axis (*x*, *y*, *z*).

Once the axes are defined, a simulation of the SFG intensity as a function of the molecular orientation is performed. In this analysis, a simulation of the intensity ratios for the different polarization combinations is compared with the experimental intensity ratios to determine the molecular orientation, as seen in Figure 8. For a methyl of an alkyl chain, a free rotation about the C_3 axis is assumed. Consequently, its orientation is described with respect to its tilt (θ) angle. On the other hand, the ring orientation is described by the tilt (θ) as well as by the twist (φ) angle.

Since SFG probes vibrations with polar ordering, the absence of the C(2)−H stretch and the symmetric H−C(4)C(5)−H peaks indicates that the dynamic dipole projection of the ring is parallel to the surface plane. In other words, the ring has a tilt of 90° to the surface normal. Even with its dipole projection along the surface plane, the imidazolium ring has a possible 90° twist (φ) around the C_2 axis projecting the H−C(4)C(5)−H antisymmetric mode along the surface normal.

For a pure C_{2v} symmetry, the SFG intensity for the antisymmetric B_2 mode should be zero for all possible twists.[46] However, for this analysis, various considerations should be taken in the determination of the molecular orientation at the interface. First, consider that the molecular symmetry for the imidazolium ring H−C(4)C(5)−H is a combination of the local C_{2v} with the real C_s symmetry of the molecule. Therefore, it is possible that the H−C(4)C(5)−H (asym) of the molecule will be seen in the SFG spectra for a tilt other than 0°. In fact, this peak has been observed previously by our group for ionic liquids

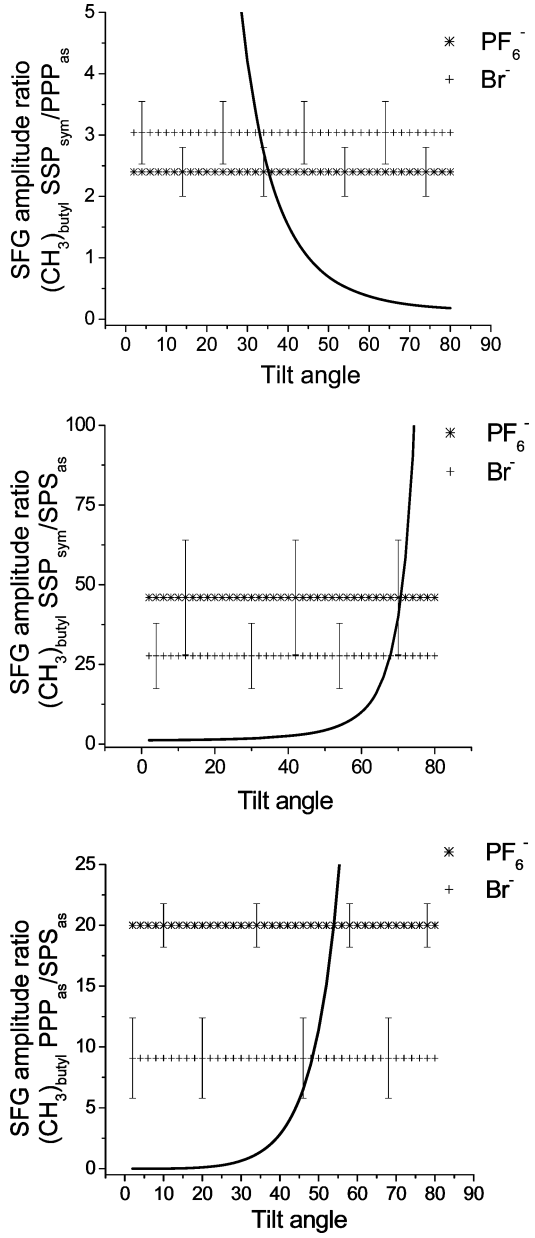

Figure 8. Simulation of the orientation of the methyl from the butyl chain assuming free rotation of the C_3 axis. Experimental results are presented as dashed lines with the standard deviation as the error lines.

with higher concentrations of water than the one presented in this analysis.[26]

Another point considered for the ring orientation is the peaks arising from N−CH_3 (sym). Small changes in the twist of the imidazolium ring will have a larger effect on the orientation of the N−CH_3 than for the methyl in the butyl chain. This effect allows a correlation of the N−CH_3 peaks with the overall ring orientation. The absence of the symmetric and antisymmetric H−C(4)C(5)−H indicates that both dynamic dipole projections are along the surface plane, and therefore, the imidazolium ring plane is parallel to the surface plane. This orientation is confirmed by the absence of the N−CH_3 vibrational modes in the SFG spectra. With the ring parallel to the surface plane, the N−CH_3 (sym) is also parallel to the surface and therefore absent in the SFG spectra. Furthermore, for an ssp polarized spectra, the N−CH_3 (asym) is many times weaker than that of the symmetric[51] and therefore not observed.

From the curve fitting of the experimental data, the peak amplitudes are compared among the different polarizations. The ratios of the experimental peak amplitudes are compared with the simulated curve of the intensity ratio as a function of the molecular orientation at the interface as seen in Figure 8. With the experimental results within the signal-to-noise ratio, the cation ring is estimated as the overlap of both curves. Given the absence of any vibrational mode from the ring, its orientation is implied to be with the ring plane tilted at >70° to the surface normal, which is nearly parallel to the surface plane. This orientation can be determined, since the simulation curve is limited at 70°. An angle of 70° is hardly distinguishable from that of 90° (Figure 8); therefore, an angle between 70° and 90° cannot be specified.

TABLE 2: Values for the Amplitudes of the Peaks at the Different Polarizations

assignment	position (cm^{-1})	SSP (error)	PPP (error)	SPS (error)
		[BMIM][PF_6]		
CH_3 (sym)	2880	7.1 (0.3)	7.3×10^{-5} (0.02)	
FR	2950	7.7 (0.4)		
CH_3 (asym)	2970	−0.19 (0.06)	3.7 (0.1)	2.3 (0.2)
		[BMIM][Br]		
CH_3 (sym)	2880	7.8 (0.4)		
FR	2950	9.3 (0.6)		
CH_3 (asym)	2970	−1 (0.6)	8.1 (0.3)	3.6 (0.3)

Despite the fact that it is a common procedure to use the symmetric mode in the SFG analysis, the symmetric peak is solely present in ssp spectra. For the other polarization combinations, the symmetric peak is either absent or within the signal-to-noise ratio and therefore cannot be used in the analysis. Also, comparing the ssp symmetric with the ppp and sps antisymmetric peaks does not provide a consistent orientation analysis (Figure 8). This disagreement is due to the model used to describe the molecular hyperpolarizability, which does not take into account the perturbation due to coupling for the antisymmetric modes. The molecular hyperpolarizability is described by the bond additivity model, which takes into account the addition of each particular C−H bond. The definition of the hyperpolarizability has been described in more detail by Hirose[43,44] and Wang.[45] As a result, a comparison of the ppp and sps antisymmetric peaks was used instead. By comparing the ppp and sps experimental ratio with the simulation (Figure 8), the orientation of the butyl chain was found to be similar for the two ionic liquids. Table 2 contains the peak amplitudes for the different polarizations. The [BMIM][PF_6] butyl chain was found to have a tilt of 54° ± 1° with a free rotation around the C_3 axis assumed.[52] For [BMIM][Br], the methyl was found to have a tilt of 47° ± 2° also over all possible twists. The angle obtained using the ppp and sps ratio was corroborated by performing null angle analysis[45,53] of CH_3 (sym) for [BMIM][PF_6], which gave a tilt angle of 59°.[54] Even though the SFG analysis performed did not provide the information necessary to determine the direction at which the butyl chain is projected, it is known that ionic liquids possess a surfactant-like behavior (due to their low surface energy)[55−57] and, therefore, are believed to have the butyl chain extended toward the gas phase instead of the bulk of the liquid.

Studies of the crystal structure of imidazolium-based ionic liquids have shown small differences in the orientation of the chain with respect to the imidazolium ring for different anions.[58−61] Hardacre et al.[58] noticed a trend with the anions' ability to form a hydrogen bond for which the alkyl chain was more parallel to the ring plane as the hydrogen bond ability of the anion increased. Even though this effect was not drastic, it was observed that it mostly affected the methylene closer to the nitrogen of the ring. This difference in orientation was

proved to be taking place in the crystallization, and once the salt was liquid, variations in the temperature had only a small effect in the chain orientation.

Hardacre's results seem to agree with the SFG results. Even though the difference in H-bonding ability between PF_6^- and Br^- is enough to observe the interaction peak solely for Br^-, this interaction does not have a strong effect on the orientation of the butyl chain at the surface when the [BMIM][Br] is liquid. By comparison of the SFG spectra of [BMIM][PF_6] at 25 and 80 °C (Figure 6), the orientation is hardly affected by the temperature, similar to Hardacre's observation for the bulk structure.

These results are slightly different from those found in previous work reported by our group,[26,27] as well as those reported by Ouchi.[24,25] This difference is due to some refinement in the analysis. As part of the refinement, a refractive index of 1.2 for the interface was introduced. Values of 1.18 and 1.2 are commonly used as refractive indexes for long alkyl chains.[46,62−64] Also, the vibrational depolarization ratios from Raman spectra were used for the determination of the molecular hyperpolarizability improving the reliability of the results obtained.[51]

Surface orientation of the ionic liquids has also been investigated by Watson using ion scattering analysis,[20,21] by Lynden-Bell using atomistic simulation,[29] by Bowers using neutron reflectometry,[65] by Deutsch using X-ray reflectivity and surface tensiometry,[66] and by Ouchi who also used SFG spectroscopy.[24,25]

The ion scattering model from Watson's group has the plane of the ring parallel to the surface normal with the C(2) carbon projected toward the gas phase, which is different from the model proposed by our group with the plane of the ring perpendicular to the surface normal. If this was the case, for our system a peak at 3110 cm^{-1} from the C(2) carbon should be observed. Likewise, if the C(2) carbon was projected toward the bulk, meaning that H−C(4)C(5)−H will be projected toward the gas phase, the H−C(4)C(5)−H resonances should be seen. The absence of the C(2) C−H stretch and the H−C(4)C(5)−H peaks indicates that the C_2 axis is not projected along the surface normal but along the surface plane, which appears to be in agreement with the results of Bowers and Lynden-Bell.

Lynden-Bell's model has the C_2 axis along the surface plane (a 90° tilt) with a 90° twist of the ring plane. On the contrary, in our results, the ring plane is perpendicular to the surface plane, which means that the cation dipole has a 90° tilt with a 0° twist. The symmetry of the molecule might play an important role in the surface orientation of the cation. Therefore, the use of 1,3-dimethylimidazolium instead of 1-butyl-3-methylimidazolium might be part of the reason for the difference of the model proposed by Lynden-Bell. On the other hand, Bowers' results nearly coincide with ours by having the ring parallel to the surface plane; however, the chains form a lamellar structure.

Conclusion

Vibrational modes of the 1-butyl-3-methylimidazolium cation were identified using IR and Raman spectroscopy. Isotopic labeling confirmed the peak assignments for the different techniques. The assignment obtained from the IR and Raman was used to identify the resonances observed in the SFG spectroscopy. Only vibrational modes from the butyl CH_3 were observed for the different polarizations.

The resonances obtained for the SFG spectroscopy suggest that the 1-butyl-3-methylimidazolium cation is oriented with the imidazolium ring parallel to the surface plane projecting the butyl chain toward the gas phase for both ionic liquids studied. The methyl of the butyl chain for [BMIM][PF_6] was found to have a tilt of 54° ± 1°, while the [BMIM][Br] has a tilt of 47° ± 2°.

Acknowledgment. This project was supported by the Petroleum Research Fund and the Welch Foundation. Equipment and acquisition of the IR and Raman spectra were provided by Professor Advincula, while polarized Raman was provided by Professor Czernuszewicz. Both professors are from the Department of Chemistry at the University of Houston, Texas.

References and Notes

(1) Wasserscheid, P.; Keim, W. *Angew. Chem., Int. Ed.* **2000**, *39*, 3772.
(2) Welton, T. *Chem. Rev.* **1999**, *99*, 2071.
(3) Holbrey, H. D.; Seddon, K. R. *Clean Prod. Proc.* **1999**, *1*, 223.
(4) Dupont, J.; Suarez, P. A. Z.; Einloft, S.; Dullius, J. E. L.; de Souza, R. F. *J. Chem. Phys.* **1998**, *95*, 1626.
(5) Grätzel, M.; Bonhôte, P.; Dias, A.; Papageorgiou, N.; Kalyanasundaram, K. *Inorg. Chem.* **1996**, *35*, 1168.
(6) Huddleston, J. G.; Visser, A. E.; Reichert, W. M.; Williauer, H. D.; Broker, G. A.; Rogers, R. D. *Green Chem.* **2001**, *3*, 156.
(7) Branco, L. C.; Rosa, J. N.; Ramos, J. J. M.; Afonso, C. A. M. *Chem.—Eur. J.* **2002**, *8*, 3671.
(8) Fuller, J.; Carlin, R. T.; Osteryoung, R. A. *J. Electrochem. Soc.* **1997**, *144*, 3881.
(9) Suarez, P. A. Z.; Selbach, V. M.; Dullius, J. E. L.; Einloft, S.; Piatnicki, C. M. S.; Azambuja, D. S.; de Souza, R. F.; Dupont, J. *Electrochim. Acta* **1997**, *42*, 2533.
(10) Wadhawan, J. D.; Schroder, U.; Neudeck, A.; Wilkins, S. J.; Compton, R. G.; Marken, F.; Consorti, C. S.; de Souza, R. F.; Dupont, J. *J. Electroanal. Chem.* **2000**, *493*, 75.
(11) Bard, A. J.; Ding, Z.; Moulton, R.; Quinn, B. M. *Langmuir* **2002**, *18*, 1734.
(12) Rogers, R. D.; Huddleston, J. G.; Williauer, H. D.; Swatloski, R. P.; Visser, A. E. *Chem. Commun.* **1998**, 1765.
(13) Sheldon, R. *Chem. Commun.* **2001**, 2399.
(14) Grätzel, M.; Zakeeruddin, S. M.; Exnar, I.; Wang, P. *Chem. Commun.* **2002**, 2972.
(15) Anthony, J. L.; Maginn, E. J.; Brennecke, J. F. *J. Phys. Chem. B* **2002**, *106*, 7315.
(16) Cadena, C.; Anthony, J. L.; Shah, J. K.; Morrow, T. I.; Brennecke, J. F.; Maginn, E. J. *J. Am. Chem. Soc.* **2004**, *126*, 5300.
(17) Kim, Y. J.; Cheong, M. *Bull. Korean Chem. Soc.* **2002**, *23*, 1027.
(18) Buzzeo, M. C.; Klymenko, O. V.; Wadhawan, J. D.; Hardacre, C.; Seddon, K. R.; Compton, R. G. *J. Phys. Chem. B* **2004**, *108*, 3947.
(19) Camper, D.; Scovazzo, P.; Koval, C.; Noble, R. *Ind. Eng. Chem. Res.* **2004**, *43*, 3049.
(20) Watson, P. R.; Gannon, T. J.; Law, G.; Carmichael, A. J.; Seddon, K. R. *Langmuir* **1999**, *15*, 8429.
(21) Watson, P. W.; Law, G. *Chem. Phys. Lett.* **2001**, *345*, 1.
(22) Katayanagi, H.; Hayashi, S.; Hamaguchi, H.; Nishikawa, K. *Chem. Phys. Lett.* **2004**, *392*, 460.
(23) Bowers, J.; Vergara-Gutierrez, M. C.; Webster, J. R. P. *Langmuir* **2004**, *20*, 309.
(24) Sung, J.; Jeon, Y.; Kim, D.; Iwahashi, T.; Iomori, T.; Seki, K.; Ouchi, Y. *Chem. Phys. Lett.* **2005**, *406*, 495.
(25) Iimori, T.; Iwahashi, T.; Ishii, H.; Seki, K.; Ouchi, Y.; Ozawa, R.; Hamaguchi, H.; Kim, D. *Chem. Phys. Lett.* **2004**, *389*, 321.
(26) Baldelli, S. *J. Phys. Chem. B* **2003**, *107*, 6148.
(27) Rivera-Rubero, S.; Baldelli, S. *J. Am. Chem. Soc.* **2004**, *129*, 11788.
(28) Rivera-Rubero, S.; Baldelli, S. *J. Phys. Chem. B* **2004**, *108*, 15133.
(29) Lynden-Bell, R. M. *Mol. Phys.* **2003**, *101*, 2625.
(30) Talaty, E. R.; Raja, S.; Storhaug, V. J.; Dolle, A.; Carper, W. R. *J. Phys. Chem. B* **2004**, *108*, 13177.
(31) Wilkes, J. S.; Dymek, C. J.; Heimer, N. E.; Rovang, J. W.; Dieter, K. M. *J. Am. Chem. Soc.* **1988**, *110*, 2722.
(32) Welton, T.; Cammarata, L.; Kazarian, S. G.; Salter, P. A. *Phys. Chem. Chem. Phys.* **2001**, *3*, 5192.
(33) Fitchett, B. D.; Conboy, J. C. *J. Phys. Chem. B* **2004**, *108*, 20255.
(34) MacPhail, R. A.; Strauss, H. L.; Snyder, R. G. *J. Phys. Chem.* **1984**, *88*, 334.
(35) Snyder, R. G.; Aljibury, A. L.; Strauss, H. L.; Casal, H. L.; Gough, K. M.; Murphy, W. F. *J. Chem. Phys.* **1984**, *81*, 5352.
(36) MacPhail, R. A.; Strauss, H. L.; Snyder, R. G. *J. Chem. Phys.* **1982**, *77*, 1118.
(37) Hill, I. R.; Levin, I. W. *J. Chem. Phys.* **1979**, *70*, 842.
(38) Carter, D. A.; Pemberton, J. E. *J. Raman Spectrosc.* **1997**, *28*, 939.
(39) Buck, M.; Himmelhaus, M. *J. Vac. Sci. Technol., A* **2001**, *19*, 2717.

(40) Shultz, M. J.; Schintzer, C.; Simonelli, D.; Baldelli, S. *Int. Rev. Phys. Chem.* **2000**, *19*, 123.
(41) Bain, C. D. *J. Chem. Soc., Faraday Trans.* **1995**, *91*, 1281.
(42) Huang, J. Y.; Shen, Y. R. *Sum Frequency Generation as a Surface Probe*; World Scientific: Singapore, 1995; Vol. 5.
(43) Hirose, C.; Akamatsu, N.; Domen, K. *J. Phys. Chem.* **1992**, *96*, 997.
(44) Hirose, C.; Akamatsu, N.; Domen, K. *Appl. Spectrosc.* **1992**, *46*, 1051.
(45) Wang, H.-F.; Gan, W.; Lu, R.; Rao, Y.; Wu, B.-H. *Int. Rev. Phys. Chem.* **2005**, *24*(2), 191.
(46) Lu, R.; Gan, W.; Wu, B.; Chen, H.; Wang, H. *J. Phys. Chem. B* **2004**, *108*, 7297.
(47) Wilkes, J. S.; Zawaroto, M. J. *J. Chem. Soc., Chem. Commun.* **1992**, 965.
(48) Pringle, J. M.; Golding, J.; Forsyth, C. M.; Deacon, G. B.; Forsyth, M.; MacFarlane, D. R. *J. Mater. Chem.* **2002**, *12*, 3475.
(49) Ren, R. X.; Robertson, A. PCT Patent WO/03/051894, 2003.
(50) MacFarlane, D. R.; Forsyth, S. A.; Golding, J.; Deacon, G. B. *Green Chem.* **2002**, *4*, 444.
(51) Lu, R.; Gan, W.; Wu, B.; Zhang, Z.; Gou, Y.; Wang, H. *J. Phys. Chem. B* **2005**, *109*, 14118.
(52) Hirose, C.; Yamamoto, H.; Akamatsu, N.; Domen, K. *J. Phys. Chem.* **1993**, *97*, 10064.
(53) Lu, R.; Gan, W.; Wang, H. *Chin. Sci. Bull.* **2003**, *48*, 2183.
(54) Santos, C.; Baldelli, S. In preparation.
(55) Bower, J.; Butts, C. P.; Martin, P. J.; Vergara-Gutierrez, M. C.; Heenan, R. K. *Langmuir* **2004**, *20*, 2191.
(56) Miki, K.; Westh, P.; Nishikawa, K.; Koga, Y. *J. Phys. Chem. B* **2005**, *109*, 9014.
(57) Katayanagi, H.; Nishikawa, K.; Shimozaki, H.; Miki, K.; Westh, P.; Koga, Y. *J. Phys. Chem. B* **2004**, *108*, 19451.
(58) Bradley, A. E.; Hardacre, C.; Holbrey, J. D.; Johnston, S.; McMath, S. E. J.; Nieuwenhuyzen, M. *Chem. Mater.* **2002**, *14*, 629.
(59) Holbrey, H. D.; Reichert, W. M.; Nieuwenhuyzen, M.; Johnston, S.; Seddon, K. R.; Rogers, R. D. *Chem. Commun.* **2003**, 1636.
(60) Holbrey, H. D.; Reichert, W. M.; Nieuwenhuyzen, M.; Sheppard, O.; Hardacre, C.; Rogers, R. D. *Chem. Commun.* **2003**, 476.
(61) Ozawa, R.; Hayashi, S.; Saha, S.; Kobayashi, A.; Hamaguchi, H. *Chem. Lett.* **2003**, *32*, 948.
(62) Zhuang, X.; Miranda, P. B.; Kim, D.; Shen, Y. R. *Phys. Rev. B* **1999**, *59*, 12632.
(63) Bell, G. R.; Bain, C. D.; Ward, R. N. *J. Chem. Soc., Faraday Trans.* **1996**, *92*, 515.
(64) Wang, J.; Chen, C.; Buck, S. M.; Chen, Z. *J. Phys. Chem. B* **2001**, *105*, 12118.
(65) Bowers, J. Vergara-Gutierrez, M.; Webster, J. R. P. *Langmuir* **2004**, *20*, 309.
(66) Solutskin, E.; Ocko, B. M.; Taman, L.; Kuzmenko, I.; Gog, T.; Deutsch, M. *J. Am. Chem. Soc.* **2005**, *127*, 7796.